Dust collection Strategy and Inner Morphology of Dust Particles in ASDEX Upgrade

M. Balden[1], N. Endstrasser[1], V. Rohde[1], M. Rasinski[1,2], S. Lindig[1], R. Neu[1] and the ASDEX Upgrade Team[1]

[1] Max-Planck-Insitut für Plasmaphysik, Euratom Association, Boltzmannstrasse 2, D-85748 Garching, Germany

[2] Warsaw University of Technology, Faculty of Material Science and Engineering, Woloska 141, 02-507, Poland

E-mail contact of main author: Martin.Balden@ipp.mpg.de

Abstract. The dust collection strategy in AUG is described in detail. The use of mono crystalline Si collector plates installed during the last three operation campaigns of AUG (2007-2009) is supported by filtered vacuum cleaning and collection with adhesive tape. The outer and inner morphology and elemental composition of the collected dust particles were analyzed with a scanning electron microscope equipped with an energy dispersive X-ray spectrometer (EDX) and a focused ion beam for cross-sectioning of individual particles. The majority of particles are dominated by tungsten showing basically two different types of outer appearance: flakes and spheroids. For the latter species of W-dominated particles in by fare the most cases, a solid W core is observed, which is coated with lower Z material. This results in various surface morphologies: smooth, homogeneously covered with indentations, cracked, bumpy, and covered with smaller particles. As coated W-dominated droplets show a radial homogeneity in the thickness of their adhered layers, the coating process seems to happen during the levitation phase of the particle after their solidification, i.e., inside the scrape of layer plasma. Also conglomerates of B, C, and W appear as spherical particles after their contact with plasma.

1. Introduction

Accidental air or steam ingress during operation of ITER can lead to significant production of explosive hydrogen on the reactive surfaces of accumulated dust particles and dust mobilization is possibly followed by long-range transport of radioactive nuclides embedded therein. Both scenarios are vastly influenced by morphological properties of the dust particles, such as particle size, specific surface area and elemental composition [1]. Beyond the radiological safety aspect of dust, effects of dust on the plasma performance and operation have to be considered [2]. Therefore, the dust production mechanisms, its mobilization, transport and deposition pattern have to be investigated and quantified.

Since the late 1990s particles have been collected in various devices during vents [3-5]. Starting with the ASDEX Upgrade (AUG) campaign 1999 the transition from a carbon to a full tungsten first wall was pursued and dust was collected in maintenance periods and analyzed [5-8] in order to observe the evolution of the dust composition after operation phases with different first wall configurations. Based on these investigations, a classification of sampled particles into *dust* and *debris* was proposed [8]. Particles which had plasma contact or were produced by direct plasma wall interaction processes are denoted as *dust*, whereas *debris* describes particles which are introduced into or produced in the vacuum vessel during maintenance works or produced during plasma operation by mechanical friction of moving in-vessel components.

Furthermore, in recent studies applying analytical scanning electron microscopy (SEM with energy dispersive X-ray spectrometry (EDX)), a link between size and outer morphology was

proposed. A first evaluation of a statistical relevant number of particles was analyzed regarding their composition [8,9]. For particles below 5 μm size, the probability is increased to be spherical and to have tungsten as their main constituent. Above 5 μm in diameter, complex conglomerates - dominated by carbon and boron forming an embedding matrix for smaller W particles - are the largest fraction of all particles. A classification regarding shape and composition was established in [9], and the present study follows this classification scheme. As conclusion form this classification, about 90% of all analyzed particles on Si collectors of campaign 2009 belong to the main classes: tungsten-dominated flakes (30%) and spheroids (20%), carbon-dominated flakes (30%), boron crystallites and flakes (10%) [8,9].

In this paper the strategy of dust studies at AUG is described beginning with the installed collector plates, post-mortem collection via adhesive tapes and filtered vacuum method up to the analysis procedure used for the investigation of the inner morphology of individual dust particles. The dust particles selected for detailed investigation of the inner morphology represent mainly the statistical relevant classes of W-dominated spheroids. Note the expression droplet imply that the particle was molten and spheroids classify only the shape, here used for round particles with an aspect ratio of up to 1.2 [9].

2. Dust Collection Strategy in AUG

In the past, dust particles were collected in AUG by adhesive tapes as a standard procedure after each campaign and, less frequent, by filtered vacuum cleaning. As adhesive tapes standard 3M Scotch tapes or more recently Plano-em polycarbonate tabs with 25 mm diameter mounted on standard SEM aluminium stubs were used. The adhesive tapes were simply stuck onto the in-vessel surfaces and removed. Thereafter, they were covered by a transparent plastic foil for storage. The filtered vacuum cleaning was performed using Whatman Anapore Aluminiumoxide membranes with 0.02 μm pore size and a diameter of 47 mm [5]. In the 10 filtered vacuum samplings after campaign 2009, air streaming with a flux of 5 l/min through the nozzle (a stainless steel tube with 1/8 inch diameter and 45 to 140 mm length) was used. The nozzle was held in short distance above the surface transporting the mobilized particles onto the filter mounted on the support grid of the stainless steel housing. The filter housing was attached to a 10 m long tube connecting to the membrane pump outside the vacuum vessel.

Both techniques have the disadvantage that they collect each particle class with a different efficiency strongly depending on the class-defining particle properties, e.g., their mobilization by an air stream (expressed as aerodynamic diameter) or their sticking probability (determined by surface wetting capability of the glue of adhesive tape). Especially spherical particles with a diameter less than 50 μm are collected with a strongly reduced efficiency by vacuuming in contrast to adhesive tapes. Furthermore, conglomeration of particles, destruction by deformation, abrasion, and break-up takes place. Nevertheless, both techniques allow to collect dust particles on many various positions inside the vessel. This leads to valuable data about the amount of dust and its distribution in the devices. Furthermore, both give an idea which types of dust exist, e.g., from flakes of deposition layers over fragments of cable isolation to fibres from cloth and hairs. Therefore, all investigated horizontal areas in AUG were sampled by both techniques after the 2009 campaign. First, the vacuuming nozzle was meandered in short distance across the surface and, subsequently, the adhesive carbon tabs on standard SEM sample holders were multiply pressed with gentle force onto the surface, until the complete area was covered at least once by the tab. All particles collected on these tape

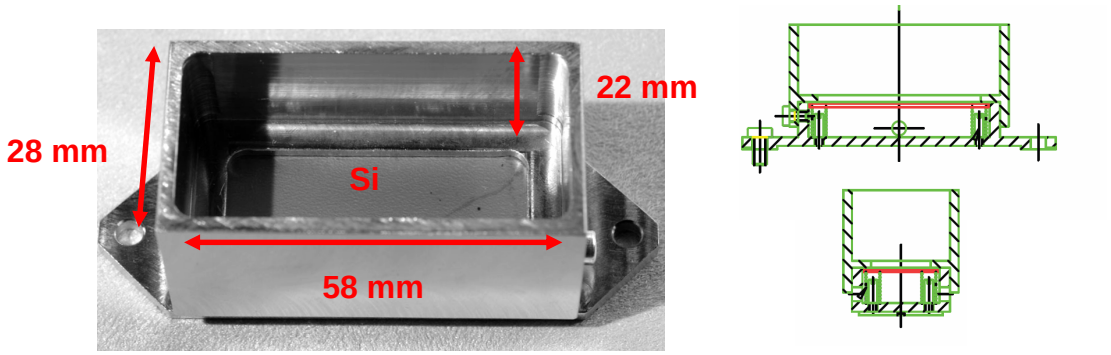

FIG. 1: Photograph and technical drawing of the stainless steel dust collector housings: the position of the silicon wafer is indicated by the diffusively reflecting plate (photo), which is pressed against the metallic frame from the bottom side.

samples are missed by the filtered vacuum cleaning, i.e., they give information about the collection efficiency and selectivity of filtered vacuum cleaning.

Since the campaign 2006, collector plates with a specially designed holding structure are installed in AUG. As a first try (campaign 2006), glass plates were used as collector plates, but due to the composition of the glass, the element analysis using EDX was hindered. Therefore, mono crystalline Si plates available as wafer from the industry are used since 2007. As the wafers are mechanically more sensitive, the holder had to be re-constructed. The final design used is shown in Fig. 1. The wafer is pressed to the upper part by a spring. A large contact area reduces the stress on the wafer. A box above the wafer prevents that the collected dust is removed during the vent of the vessel. An additional cap can be mounted on top of the box. This is removed by the last people leaving the vessel before the closing and mounted by the first people after the opening. So the contamination of the wafer is strongly reduced.

The advantages of these collectors are that only particles mobilized during plasma operation and not during maintenance phases arrive on the plates. Furthermore, it could be expected that all types of arriving particles stay on them, i.e., no selection by the collection. Due to the Si as substrate, the analytical SEM analysis works very well. Additionally, the history of particles could be reconstructed in some cases by investigation of their surrounding on the collector [6]. The main disadvantages of this method are that the collection positions have to be selected before the experimental campaign, that only locations without plasma contact and low power load can be chosen, and that only a limited number can be installed. The five installed collector in the last campaigns are poloidally and toriodally distributed in order to obtain the spreading of the dust particles [6,8,9].

After the campaign 2009, additional filtered vacuum cleaning was performed around one of the 5 installed dust collectors and, subsequent, further dust was collected with adhesive tapes on the same areas. The comparison of the results from the Si collector plates to the pair filter plus tape will lead to an overall efficiency assessment. A statistical analysis of the 5 Si collector plates of the campaign 2009 is given in [9] leading to a classification of W-dominated spheroids, W-, C-, B-dominated flakes and others. The analysis of the collected 10 sample pairs filter-tape is still ongoing and will be published in a future paper.

3. Dust Analysis Strategy

In order to obtain information on the outer and inner morphology of individual dust particles and their chemical composition, the "Helios" device at IPP is used (HELIOS NanoLab 600, FEI). This device combines a SEM with a field emission electron gun and a focused ion beam (FIB) microscope with an inclination angle between the two beams of 52°. This allows cross-sectioning of dust particles with the FIB and imaging with the SEM, even during cutting. Additionally, the device is equipped with an EDX (Oxford Inka System with Features Option). The automated EDX software takes SEM images and detects individual dust particles of a minimal size (see below) by grey-scale threshold analysis of these images. It records an EDX spectrum of each detected particle, analyzes these spectra, and generates a database with an icon of each particle, some geometrical data (e.g. area and perimeter) and its chemical composition. Automatically the selected area (e.g. 2×2 mm^2) is segmented into an appropriate number of field of view area (e.g. 13×12 μm^2) and scanned by the SEM at a chosen, higher magnification. A size filter is applied, e.g., particles with a size less than 16 pixel, which corresponds to an equivalent circle diameter (ECD) of 0.28 μm, are not registered. With this automated SEM/EDX analysis method easily more than 10000 particles per collector sample are registered and characterized within one weekend. The database allows classification and statistical analysis of the investigated ensemble of dust particles [9].

As the position of each particle is also stored, subsequently, some selected particles of each class are imaged in high resolution and a subgroup of these is then cross-sectioned. Note that the classification by the automated system can be refined by analyzing particles in more detail. For cross-sectioning, lamella fabrication and to extract individual particles for further analysis, a nano-manipulator system combined with the possibility of depositing Pt-C-coatings is available. The analysis of the inner morphology allows conclusions about the origin and history of the dust particles. Furthermore, the classification from the outer morphology can be confirmed.

4. Results on Cross-sectioned Spherical Dust Particles

The outer and inner morphology of more than hundred spherical W-dominated dust particles was analyzed in more detail. Note that for the sub-micron particles, a larger fraction belongs to the class of flakes and are excluded further on. The outer surface of the W-dominated spheroids varies between smooth, bumpy with hills and groves, cracked like dried soil, to inhomogeneous composed with other particles attached (see Figs. 2-4). The smooth ones are by fare the most frequent ones, roughly three quarters of all W-dominated spheroids. In addition, a few unique particles are observed (Fig. 3).

Two individual W-dominated spheroids with distinct different outer morphology are shown in Fig. 2. The cross-sectioning exhibits that the core of both particles is composed of solid tungsten. The origin of the spherical W droplet is expected to be from arcing, which ejects molten tungsten [8,10]. The surface morphology is determined by the coating, which completely covers the spheroid. The uniform thick shell around this particle indicates that the coating process occurred during levitation. Alternatively, a step-wise coating process occurred during frequent mobilization events, which is very unlikely. Note that the grainy deposition observed on the Si substrate (Fig. 2c) could also be present on the particles affecting the outer morphology of the top side of the particle. Nevertheless, it is most reasonable that the coating dominantly happened inside the scrape of layer plasma.

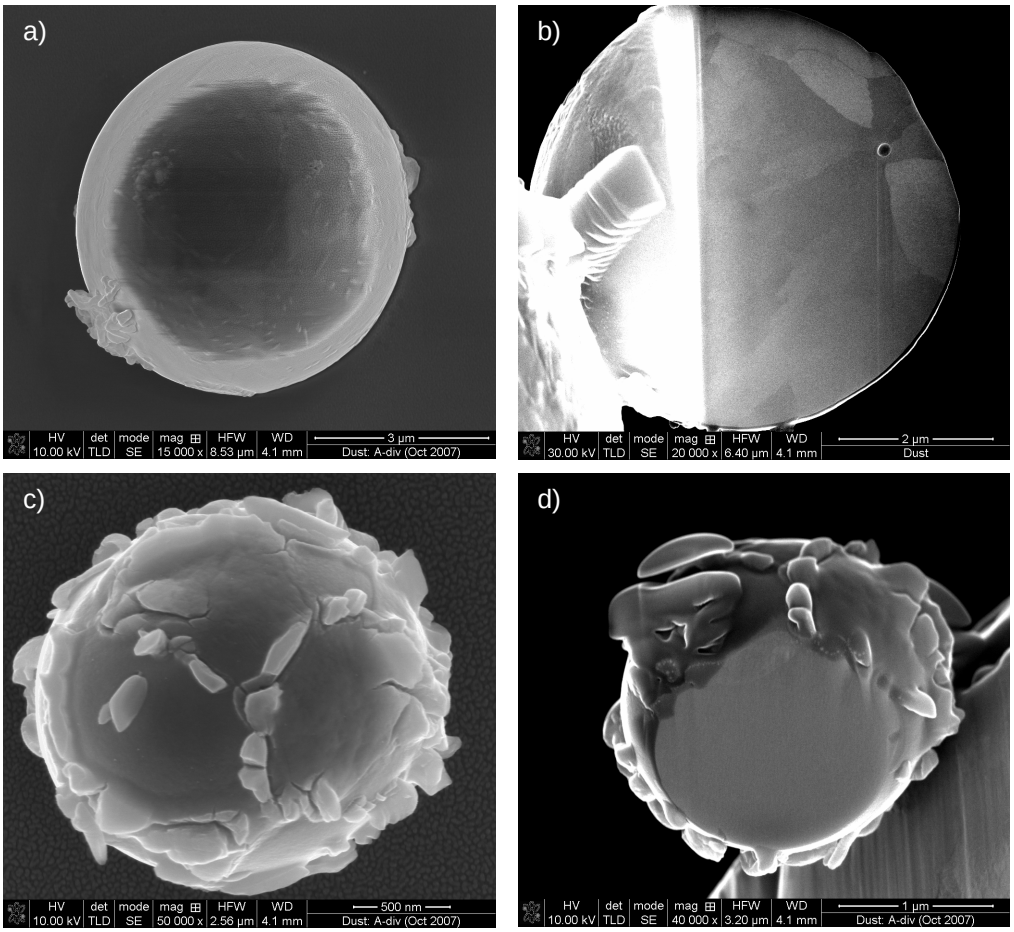

FIG. 2: a) SEM image of a W droplet of ~6 µm in diameter with some surface roughness and attached material (on Si collector plate). b) The same particle shown in a) after transferring it onto a Cu TEM-grid (left border) and thinning its right half to electron transparency. Clearly the internal W grain structure after solidification and a thin layer at the outer edge is visible. c) SEM image of a W droplet of ~2 µm in diameter with some surface cracks and attached material (on Si collector plate, which shows a fine grainy deposition). d) The same particle as shown in c) after transferring it onto a Cu TEM-grid (right lower part) and cross-sectioning.

The W core of such W-droplets usually consists of several W grains with a few pores of a size of 20-100 nm (Fig. 2b). It could be assumed that the pores are formed during the solidification of the molten W droplet and the nucleation of several grains.

Figure 3 shows a unique particle with some regular surfaces. EDX mapping on its cross-section exhibits that the regularly shaped boron-dominated crystallites are surrounded by tungsten oxide. The oxide has porous structure. The building process of that particle is unknown.

Figure 4 shows another spherical particle which was definitely passing the scrape of layer plasma and is classified as a W-dominated spheroid, too. The spherical shape is assumed to be due to ablation of material while passing the plasma. This particle is a conglomerate of W droplets embedded in a carbon-boron matrix (see below and Fig. 2 of [8]). Its composition is quite inhomogeneous. While the bright areas are strongly dominated by W, the dark ones contain much more boron (Fig. 4). Overall, the tungsten content dominates the particle.

Similar composition variations are observed on the fragile flake shown in Fig. 5. This particle is classified as a W-dominated flake. The analysis of many W-, C-, and B-dominated flakes

leads to the conclusion that a significant fraction of all flakes are in principle of the same material conglomerate, which only differ in the amount of each element. I.e., they should have the same origin: re-deposited material, which flaked away, e.g., by thermal stresses during arcs, transient power loads and disruptions (see [7,8]). Figure 6 shows the surface of an AUG divertor tile, which suffers to high arcing activity. Beside the arc track, flaked material is observed. It is composed by subsequent deposition from the plasma and arcing activity in its vicinity, which splashes molten tungsten. The surface morphology of this flaked material (Fig. 6c) is equal to W-, C-, and B-dominated flakes (Fig. 5). It is assumed that a fraction of this flaked material arrives at the collectors without plasma contact, as the fragile structure observed on many individual particles supports (Fig. 5), while some other fraction passes the plasma without ablating completely and ending in such spheroids as shown in Fig. 4.

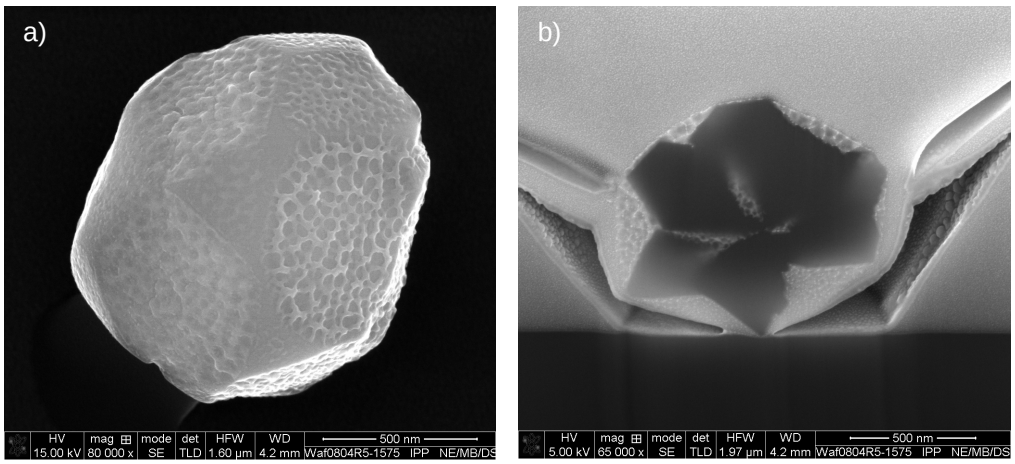

FIG. 3: a) SEM image of a unique, nearly spherical particle with some regular surfaces and some porous looking structure. b) Cross-section image of the particle of a) after covering with a Pt-C coating (bright part). The Si collector plate is visible (dark, lower part of the image), while the boron-dominated core (dark star-like structure) is surrounded by tungsten oxide visible as porous structure in a). Note the large pores are artefacts of the Pt-C coating.

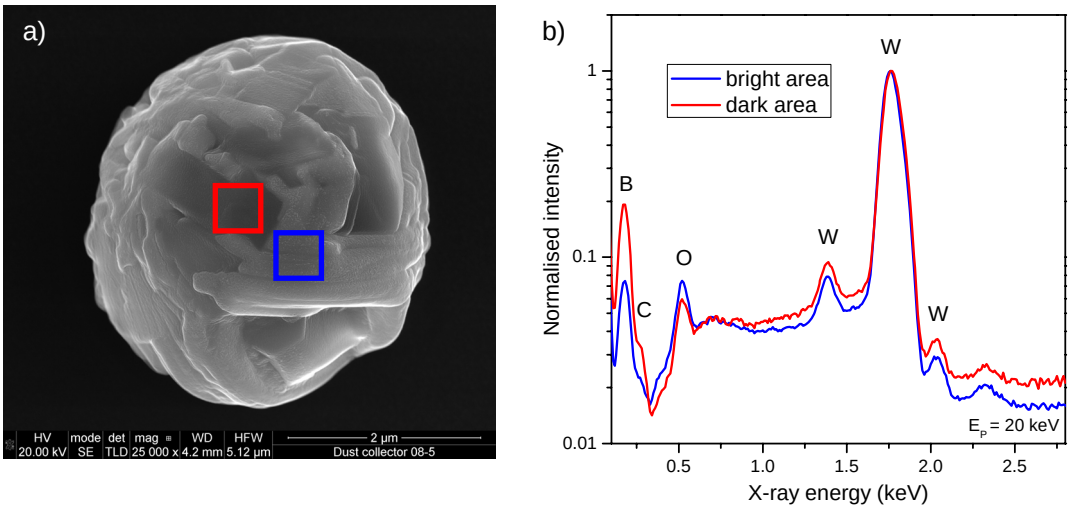

FIG. 4: a) SEM image of a W-dominated ball of about 8 µm in diameter with some dark and bright area (on the Si collector plate). b) EDX spectra of the two marked areas normalised to the main W peak (1.76 keV). Clearly the strong increase of the boron signal for the dark region is visible. The strong signal of W in the dark area is explained by the penetration and spreading of the 20 keV of the primary electron beam.

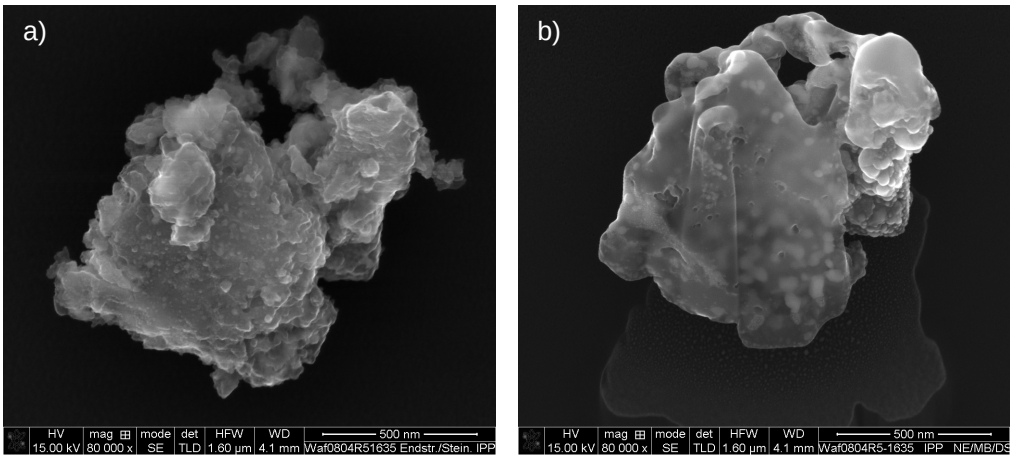

FIG. 5: a) SEM image of a W-dominated conglomerate flake on the Si collector plate and b) partly cross-sectioned. The shadow of the particle on the Si due to the scanning with the FIB (lower part of the right image) allows an estimation of the particle height, which is in this case ~500 nm. Note the 30 keV Ga ion beam damages the fragile structure, as can be seen from the comparison of the particle surface in both images (top part of the particle).

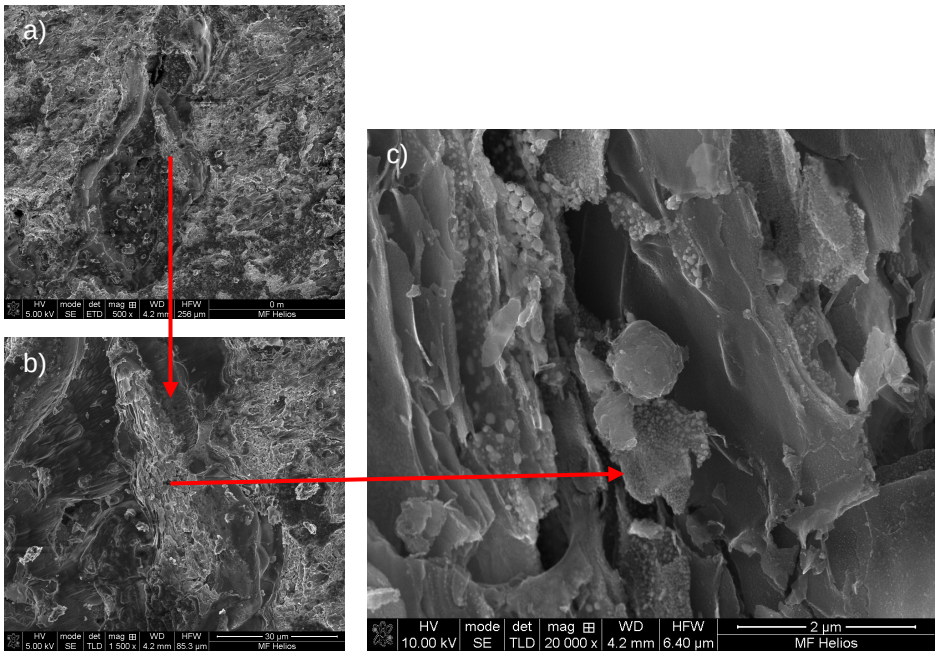

FIG. 6: SEM images of the surface of an AUG divertor tile, which suffers strong arcing. a) Overview with large arc track, b) edge of the arc track in medium magnification, and c) detail view of the partly flaked co-deposited layer beside the arc track.

All together, more than 90% of all W-dominated spheroids are W droplets, counting the smooth W spheres together with the particles which show coating and attached particles homogeneously around them, indicating their direct plasma contact. The W droplets are expected to be produced by arcing. They are found all around the whole torus. Also the conglomerate of W droplets in C-B matrix mobilised by arcs are widely distributed in the torus.

5. Conclusion

The dust collection strategy in AUG allows to obtain statistical relevant data leading to a classification scheme [9]. This scheme could be refined by analysing the inner morphology of individual particles of each class. The present analysis focuses on the W-dominated spheroids and touches marginally the W-, C-, and B-dominated flakes.

More than 90% of all W-dominated spheroids are W-droplets presumably originated from arcs. Further more, at least about a quarter of all W-dominated spheroids have passed the scrape of layer plasma. All together, it is reasonable to generalize the properties of all particles of the class "W-dominated spheroids" for safety assessment as ideal spheres composed only of W, i.e., minimal surface area by high density. This situation is significantly different for the flakes with their dramatic larger surface area and their low density. More work is necessary on these classes of dust with an expected strong refined of their classification. As first result, a part of all flakes are conglomerate of W-droplets embedded in C-B matrix, which are originated by flaking off of deposited films from areas with strong arcing activity. Note that the thickness of deposited films in AUG is strongly reduced since switching to a full W first wall [11].

Further evaluation of the dust collected on filters and adhesive tapes will allow determining the collection efficiency of the different collection methods.

References

[1] MCCATHY, K.A., *et al.*, "The safety implications of tokamak dust size and surface area", Fusion Eng. Des. **42** (1998) 45.
[2] Roth, J., *et al.*, "Recent analysis of key plasma wall interactions issues for ITER", J. Nucl. Mater. **390-391** (2009) 1.
[3] CARMACK, W.J., *et al.*, "Characterization and analysis of dusts produced in three experimental tokamaks: TFTR, DIII-D, and Alcator C-Mod", Fusion Eng. Des. **51** (2000) 477.
[4] CARMACK, W.J., *et al.*, "Collection and analysis of particulate from the DIII-D Tokamak"; Fusion Eng. Des. **39** (1998) 477.
[5] SHARPE, J.P., *et al.*, "Characterization of dust collected from ASDEX-Upgrade and LHD", J. Nucl. Mater. **313-316** (2003) 455-459.
[6] ROHDE, V., "Demonstration of Diagnostic Techniques for time resolved Dust Measurement in Tokamaks", TW6-TPP-DUSMEAS EFDA Final Report (2008).
[7] BALDEN, M., ROHDE, V., ASDEX UPGRADE TEAM, "First investigation of the inner morphology of dust particles from ASDEX Upgrade", Post-deadline poster at 18th Int. Conf. on Plasma Surface Interactions (2008), Toledo, Spain.
[8] ROHDE, V., BALDEN, M., LUNT, T., ASDEX UPGRADE TEAM, "Dust investigations at ASDEX Upgrade", Phys. Scr. **T136** (2009) 014024.
[9] ENDSTRASSER, N., *et al.*, "Video tracking and post-mortem analysis of dust particles from all tungsten ASDEX-Upgrade", (Proc. 19th Conf. on Plasma Surface Interactions (2010), San Diego, USA), J. Nucl. Mater., in press.
[10] ROHDE, V., *et al.*, "Tungsten Erosion By Arcs In ASDEX Upgrade", (Proc. 19th Conf. on Plasma Surface Interactions (2010), San Diego, USA), J. Nucl. Mater., in press.
[11] SUGIYAMA, K,. et al., "Deuterium inventory in the full-tungsten divertor of ASDEX Upgrade", Nucl. Fusion **50** (2010) 035001.